Floor vibration serviceability in a multistory factory building

James MW Brownjohn
College of Engineering, Mathematics and Physical Sciences, University of Exeter, UK

Tso-Chien Pan
College of Engineering, Nanyang Technological University, Singapore

Christopher Middleton
Xodus Group, Southampton, UK

Su Chern Tan
JTC Corporation, Singapore

Weifeng Yuan
College of Engineering, Nanyang Technological University, Singapore

Guichang Yang
College of Engineering, Nanyang Technological University, Singapore

Contact author: Professor James Brownjohn
Vibration Engineering Section
CEMPS
University of Exeter
Harrison Building, North Park Road
Exeter EX4 4QF
E-mail: J.Brownjohn@exeter.ac.uk
+44 01392 723698

Abstract

Experimental and analytical modal analysis and in-operation vibration measurements were performed on the massive concrete structural floors of several structurally connected 'units' of a six-level, multi-tenant industrial complex with total floor usable area exceeding $0.1km^2$. The aim of the systematic study was to characterise vibration sources and factors that affect vibration serviceability, which is a major concern when changing usage patterns lead to conflicting requirements for vibration generation and tolerance for different types of industrial/commercial user. This was a rare investigation aiming to provide information on specific performance and relevant technologies for occupancy decisions by tenants and building management of similar structures.

Floors evaluated were within different types of industrial single-occupant unit stacked up to six levels and having multi-bay floors with spans up to 12m with first vibration mode frequencies greater than 8Hz. These 'high frequency floors' display typical transient response behaviour to footfalls, with response levels controlled by modal mass.

Units were studied in typical operational conditions including warehousing, instrument assembly and testing, light electronic/mechanical manufacturing and machining. Vibration sources included internal and external vehicles, human footfalls and machinery.

The study showed the most onerous form of loading to be forklift trucks and that higher level floors of the same type were least serviceable. Experimental modal analysis showed a surprising range of modal properties for nominally identical floors of the same type and the relevance to performance of modal mass.

Keywords: vibration serviceability floor modal test footfall machinery forklift

Vibration serviceability of industrial floors in Singapore

In Singapore and other rapidly developing economies in Asia, small local and foreign companies representing a wide range of industries from light manufacturing through to precision electronics are concentrated in multi-tenant industrial parks such as the one studied in this paper. These are often very large single structures with spacious units at several levels and allowing for direct vehicle access. With a shift away from more traditional manufacturing industries to light high-technology fabrication, testing and services, changes in usage result in changing vibration serviceability requirements which may conflict with vibration generating activities of neighbors. To avoid such conflicts, some form of vibration rating could be used to inform potential tenants. An ideal candidate is the vibration criteria (VC) rating system used in design of facilities accommodating vibration-sensitive test or manufacture equipment e.g. for microelectronics production.

Following the collapse of the Hotel New World in Singapore in 1986 (SCOSS, 1988), local building designs have tended to be conservative and face very strict legal requirements on construction and safety. While structural safety is properly addressed, vibration serviceability is usually assumed to be satisfactory, which is typically the case with the heavy cast in-situ or precast concrete construction typically used for industrial parks. The result is that vibration serviceability assessments of the massive and stiff floors will rate them as ‘high frequency’ i.e. not capable of experiencing resonance due to human footfalls (Wyatt, 1989, Pavic and Willford, 2005).

However, even for such high frequency floors, good vibration performance is not guaranteed and problematic vibration performance does occur. Unfortunately due to commercial sensitivities, studies of specific structures published in peer-reviewed journals that describe both vibration measurements and modal testing are scarce and provide little detail (Brownjohn & Pavic 2006). What is available mostly relates to generic design and performance of microelectronics facilities (Amick et al., 1991).

Much more is known in relation to vibration performance of high profile structures like footbridges (Dallard et al., 2001), stadia (Rogers & Thompson, 2000) and gymnasia (Rainer & Swallow, 1986) and there is a comparative wealth of literature on the effect of high speed and underground railways on building vibrations (Xia et. al, 2009). This paper is a rare opportunity to report on vibration performance of a complete multi-use building, the means for assessing it, the factors affecting it and the implications for occupants.

S1 Complex

The S1 complex (Figure 1-3) is a structurally connected array of two-level industrial units stacked up to a total of six levels (plus mezzanines) that in Singapore is sometimes referred to as a stack-up factory (Pan and Mita, 2001). In this example there are 90 two-level industrial units with a total usable floor area over $0.1km^2$ arranged over six levels in blocks structurally and logistically connected by spiral ramps and wide access roadways. These provide heavy vehicle access to the first, third and fifth levels i.e. to the lower levels of each unit.

S1 is divided into T1000, 42 T2000, and 24 T3000/5000 units, the numbers indicating the gross floor area for each unit. T1000s are arranged in two terraces each with twelve units (left side of Figure 1) and T2000 units are arranged in seven blocks of semi-detached (adjoining pair or duplex) stacked units (top row of units in Figure 1). The T5000/3000 units are arranged in four blocks of two adjacent but detached (stand alone) stacked units (lower row of units in Figure 1). These are the largest units, with footprint of 74m×36m and comprise a two-level T5000 unit with two smaller footprint two-level T3000 units stacked on top. T3000s lose interior area to an external car park at lower levels (3 and 5) only.

Figure 2 shows a vertical section through a T5000+T3000+T3000 six-level stack in the long (74m) axis of the units, with the driveways shown at the right.

While the unit type (1000/2000/3000/5000) refers to the nominal gross floor area in m^2 over the two levels, the maximum usable floor space is somewhat less. For example T5000 usable area at ground level is $2100m^2$.

Column heights range from 6.2m to 8.4m, with spans and bay sizes depending on type. In all units, continuous reinforced concrete columns support one-way spanning main beams, with 1.2m wide precast pre-tensioned hollow core planks of varying depth forming the floors.

Floor details

Eight of the 90 units were available for evaluation of vibration serviceability, subject to occupant permission and suitability. Both levels in two of the units were assessed, providing a total of ten floors, each of which comprised multiple bays. Two T1000 floors were also studied but due to their unremarkable (and satisfactory) performance they are not reported here. In fact such units should be the best choice for vibration sensitive activities.

Table 1 summarises the ten floors and their usage while Figure 4 shows examples in operation and/or during testing. To identify the floors, the first number is the unit type, the second number is the roadway level (1, 3 or 5) and the letter L/U indicates lower or upper level. To provide a unique identification a tenant number is appended. Hence 2000-5U-6 is the upper floor of the T2000 unit having street address identified as level 5 and occupied by tenant 6.

Table 1 also provides performance information discussed in the paper e.g. the experimentally observed natural frequency of the lowest vibration mode or modes relevant to the response observations. The nature of ‘low modes’ and ‘high modes’ is described later, but all modes have frequencies exceeding 9Hz, and display transient rather than resonant response to footfalls. This type of response is the defining feature of a ‘high frequency’ floor (Brownjohn & Middleton, 2009).

Since all but one of the units reported here are T3000 and T2000, architectural plans of exemplar units are provided in Figure 5 and Figure 6.

The T3000 lower floor (Figure 4b and Figure 5) has internal 6m and 18m bays spanned by 1.2m deep main beams at 7.5m intervals (partial detail of Figure 15). The external car park for levels 3 and 5 (the lower of the two levels in each T3000 unit) is a 12m span that is usable internal floor space in T5000 units that take levels 1 and 2. Precast (typical) 0.3m deep × 1.2m wide precast hollow core planks span the 7.5m bays between main beams, and 80mm concrete topping incorporating welded mesh reinforcement provides continuity throughout. Concrete is typically Grade 50.

For T2000 units (Figure 6 and Figure 3b) the orientation of main beams and planks is rotated 90° compared to T3000. Main beams are typically 1.1m deep and span 12m or 9m while (typical) 0.38m × 1.2m planks span up to 12m.

External walls are masonry construction and are expected to provide limited vertical constraints to main beams while full height partitions were not used in any of the units tested. Hence the floors should behave structurally as systems of one-way beams continuous over column supports with simply supported planks acting as secondary beams and topping providing some composite action in both directions.

Dynamic testing and experimental modal analysis (EMA)

Modal tests, of eight of the ten floors, used single input/multiple output (SIMO) procedures (Ewins, 2000) referenced in UK design guidance for floor vibration serviceability (Steel Construction Institute 2009). This approach was chosen due to reliability required for the (ultimate) commercial application of the testing. In each case the roving hammer procedure was used, where accelerometers remained at fixed locations as an instrumented hammer was roved around test (measurement) points on the floor. A battery operated system comprising a four channel 24-bit NI USB-9233 driving three Endevco 7754-1000 IEPE accelerometers and an instrumented PCB hammer was used to provide sufficient data for modal analysis including partial mode shapes.

In addition, a detailed investigation of 2000-3L-4 to recover a full set of mode shapes over all bays used a long stroke shaker (APS400), Data Physics Quattro 4-channel 24-bit spectrum analyser and four Allied Signal QA700 servo-accelerometers.

The global rational fraction polynomial (GRFP) method (Richardson and Formenti, 1982) for system identification implemented in MODAL software (Brownjohn et al., 2001) and ME'scope software (Vibrant Technology Inc., 2003) was used for the shaker test data. GRFP and circle-fitting (Ewins, 2000) implemented in MODAL were used for the for hammer test data.

Frequency response function (FRF) measurements from all tested floors are summarized in Figure 7 plotted as absolute values of the inertance. Inertance (also known as accelerance) is the ratio of acceleration to force and has units of mass^{-1} and the examples in Figure 7 are the case where the excitation and measurement point are at the same location (or driving point) in the middle of a bay where mode shapes are expected to be largest.

System identification by GRFP curve fitting provided estimates of mode frequency, damping and mass, with numerical values summarised in Table 1.

What is immediately obvious from the two plots of Figure 7 is the varied performance of the nominally identical T2000 floors, despite their nominal similarity, compared to the similarities in the T5000/3000 floors. Also, while all floors exhibit first mode natural frequencies in the range 9-13Hz (most floors clearly show more than one mode in this range), the T5000/3000 floors have a cluster of modes in the 30-40Hz range with high point mobility values. These features are linked with modal mass values, for example the 30-40Hz T5000/3000 modes have modal masses between 28 and 45 $\times 10^3$ kg while the T2000 modes range from 45 to 180 $\times 10^3$ kg, with 2000-3L-4 having first mode masses at least twice those of the other two T2000 units. Some explanation for the two types of T5000/3000 mode and background on the T2000 performance is provided through finite element modeling.

Modal mass and damping are the most difficult parameters to identify, in particular experimental modal mass values are rarely reported, and the values presented are best estimates from a combination of system identification approaches (GRFP and circle fitting). Damping estimates are only narrowly spread for T2000 units (2.4% to 3%), similarly, but in a slightly higher range for T3000 units (2.9% to 3.8%). The lone T5000 unit has the lowest damping estimates and this is the only unit with logged complaints about floor vibrations. Generally the damping levels are consistent with values widely used in design for vibration serviceability and are unlikely to include contributions of non-structural elements that are dwarfed by the scale of the structures. As the modes occur at high frequencies and damping is not low the damping estimates should be biased significantly by classical signal processing effects of poor frequency resolution and there is no trend in values with frequency.

Vibration transmissibility between lower and upper levels within a unit

Within a stack of units there is a suspicion that vibrations can be transmitted between adjacent levels. In an experiment to check this, hammer testing was carried out on lower and upper levels of 2000-5L/U-6. The force was applied in the mid point of a 12m × 12m panel in the lower level only and the response recorded simultaneously at the same location (to obtain point mobility) and in the corresponding position on the upper floor (for transfer mobility).

Figure 8 shows the mobility (inertance) functions between the two floors and the hammer force. The two floors are far from independent: inertances are reduced by just over 50% for the upper level, and also the two floors move in antiphase, consistent with global mode involving column flexure. The frequencies given in Table 1, recovered from these functions, are the same, with no separate hammer testing on the upper level.

Finite element modeling (FEA) and analytical modal analysis

To provide insight to the dynamic behavior, several strategies were evaluated for a-posteriori finite element modeling to reconcile the experimental performance with structural characteristics. Initial models represented the one way spanning 1.2m wide planks and their much weak flexural rigidity in the transverse direction using orthotropic plate elements, but this approach could not reproduce adequately the observed dynamic characteristics. The grillage-only representation that worked best and which is briefly described here represented the cells of a hollow core unit in the main spanning direction as longitudinal beams with weaker transverse stiffness represented by small mass-less beams continuous through adjacent planks. Heights of both beam types were adjusted to include the structural effect of the topping.

For convenience, as shown in Figure 9, the beams along directions 2 and 1 are defined as primary beams and secondary beams, respectively. The width of a primary beam (direction 1) is:

$$b_1 = \frac{L_1}{N_h} \tag{1}$$

where N_h is the number of holes on the cross-section of a unit of hollow core slab. Thus, the moment of inertia of the primary beam is:

$$I_1 = \frac{1}{12} b_1 h^3 - \frac{1}{64} \pi d^4 \tag{2}$$

Assuming the transverse properties of the hollow core slab to be represented by N_s secondary beams, with N_s chosen for convenience, the width of the secondary beam is:

$$b_2 = \frac{L_1}{N_s} \tag{3}$$

The non-uniform moment of inertia of a secondary beam due to the holes is taken as the average of the two extreme cross-sections:

$$I_2 = \frac{1}{2}\left[\frac{1}{12} b_2 h^3 + \frac{1}{12} b_2 \left(h^3 - d^3\right)\right] \tag{4}$$

Hence, the depth of the equivalent solid secondary beam is:

$$h_e = \sqrt[3]{h^3 - \frac{1}{2} d^3} \tag{5}$$

To take the integral layer of topping (thickness h_t) into account the heights of both primary and secondary beams are further adjusted to h_p and h_s, which are given by Eq. (6) and Eq. (7), respectively.

$$h_p = h + h_t \quad (6)$$

$$h_s = h_e + h_t \quad (7)$$

The material of the two types of beams is assumed to be linear elastic and to take account of the steelwork, hence an equivalent Young's modulus of a reinforced concrete section is computed based on the following equivalence:

$$E_{RC} = \frac{A_C E_{Cq} + A_S E_S}{A_C + A_S} \approx E_{Cq} + \frac{A_S}{A_C} E_S \quad (8)$$

where A_C= Area of concrete cross-section, A_S= Area of the cross-section of rebars, E_S= Young's modulus of steel and E_{Cq}= Dynamic Young's modulus of concrete. Uncracked properties were used in the modeling, an approach used in vibration serviceability assessment of footbridges (Highways Agency, 2001).

Using ABAQUS, models of the different floors types tested were created, having first checked that models including all six levels but with low resolution did not result in significant changes in predicted modes. The final models were limited to a single level with fixed-ended half columns above and below, with no contribution from non-structural walls.

Comparison of EMA and FEA modal characteristics

The aim of the FEA was to expand the limited picture of dynamic behaviour revealed by the modal testing. While it was possible to estimate mode shapes experimentally for a relatively fine grid covering most of 2000-3L-4 floor area, for other units the time and operational constraints restricted FRF measurements to a few points along bay midlines covering full length and width of the unit in one or both directions. Because of incomplete matching of nodes between test and analysis, and because of the relatively small number of clearly identified and relevant modes, matching was done visually. Modal assurance criterion (Ewins, 2000) does not provide additional insight with the type of mode shape evident with these floors and was not used. Modal mass was available only for experimental modes.

T2000 floors

Figure 10 shows the excellent correspondence among the first two modes identified by FEA and EMA, both characterised by motion in the wider bay with 12m-spanning hollow core slabs. The node lines correspond with (dashed) column-lines indicated in the right hand unit of Figure 6 and point A in the figure is also indicated in Figure 6.

T5000/3000 floors

Figure 11 shows the two lower frequency FEA modes for 3000-3L-8 along with EMA frequencies. The partial experimental mode shapes (not shown) compare well with the FEA shapes and indicate that these modes engage the whole 18m bay with half-sine pattern in main beam direction and increasing number of nodal points in the 7.5m bay direction. EMA shows that the jump to lower modal mass for modes above 30Hz occurs when 18m main beams appear to accommodate a whole sine wave mode shape.

Even with the constraints of partial experimental mode shapes it is clear that the FEA reproduces the nature of the experimental modes well enough. This means that the dynamic performance of the floors is an apparently simple result of the principal bending characteristics of the main beams and planks.

Although mode shapes and frequencies correspond, there is a problem with the modal (or generalised) mass estimate for unit 2000-3L-4 being much larger than values for other T2000 floors. Experimental estimates for the two lower modes obtained from the GRFP procedure for both hammer and shaker testing agree with each other and with estimates from simpler circle-fitting and are consistent with the lower peak in the FRF of Figure 7.

An estimate of experimental modal mass (and likewise analytical mass, due to similar mode shape) can also be found using the area integral of squared mode shape (ϕ^2) scaled by mass density of the various structural components. Using unit-normalised mode shapes i.e. with maximum amplitude 1.0 (Brownjohn & Pavic, 2007) provides an estimate of 63×10^3 kg. This value is far lower than the experimental estimate but is close to experimental modal mass estimates for other T2000 floors. There is no obvious explanation other than hidden structural features specific to this unit, and there have been no further opportunities for experimental or analytical investigation. The large modal mass is reflected in relatively good performance of this unit in the operational performance evaluation now described.

Operational performance measurement and evaluation procedure

The main aim of the exercise was to provide a reference study on vibration levels of high frequency industrial floors according to usage, with interpretation through modal properties. Hence response measurements were made for the following conditions:

- Usual operation with a range of excitation sources including machinery and, in particular, forklift trucks.
- Controlled walking along paths such as indicated in Figure 5 and Figure 6 with prompting by metronome at specific pacing rates to allow direct comparison between units.

- Ambient response without machinery or pedestrian movement.

Measurements were made using the battery-operated system and data are presented in different forms, depending on which best describes the levels and character of response variation in time and frequency:

- Time series of accelerations, useful for showing absolute levels and for characterizing response due to walking and certain types of machinery,
- Power spectral densities varying with time and frequency (3D spectrograms) and
- One-third octave spectra of narrow-band root mean square (RMS) velocities, providing a standard performance metric by which all floors can be compared.

Response to forklift trucks (FLTs)

Information about effects of FLTs on floors is sparse, so far mostly appearing as doctoral studies in relation to low frequency floors (Eriksson, 1994; Ehland, 2010; Ehland et al., 2009). To add to this, example responses are presented for three different FLTs on three T3000 floors. Response is shown as time series and as peak-hold one-third octave spectra.

One-third octave spectra of velocities are typically used to describe and prescribe vibration environments for sensitive machines and instruments. RMS velocities are determined within one-third octave frequency bands having centre frequencies and bandwidths progressing approximately as $2^{n/3}$ (American National Standards, 1986) but taking preferred values e.g. 2Hz, 2.5Hz, 3.15Hz, 4Hz etc. The RMS values are usually obtained via discrete Fourier transforms (DFTs) of T second acceleration records converted to velocity at each spectral line. Squared line amplitudes within a band are summed and RMS values presented for all bands. Spectra can be shown as peak hold (maxima in each band over successive blocks) or as averages (in the RMS sense) over a complete multi-block record. Figure 12 shows time series and corresponding spectra for FLT activities on three floors. Vibration criteria (VC) are represented as lines identified in Figure 12a defining (above 8Hz) constant levels the lowest of which that envelopes all RMS values classifies the vibration performance of the floor, a process is described e.g. by Brownjohn & Pavic (2006). Above 8Hz the VC lines form a 2^n geometric progression from the lowest (VC-E) at 3µm/second to the highest (VC-A) at 50µm/second, with VC-C at 12.5 µm/second indicated as a thick line in the plots. The VCs and their application are defined by Amick et al., (2005). VC-E (not achieved by any of the floors studied) is the most stringent class specified for optical systems such as long-path lasers requiring ‘extra-ordinary dynamic stability’. An additional line at twice VC-A is the ISO-2631 base curve at 100µm/second (ISO, 2003) used as the vibration limit for hospital operating theatres. Only one of the three FLT response examples is completely bounded by any of the VC/ISO lines.

In the first FLT example, a diesel powered Toyota model 25 was driven along WP1 in floor 3000-3L-7, which is identified in Figure 5. This floor has a smooth epoxy surface and the FLT apparently used pneumatic front tyres. The resulting response is strong across a wide band of frequencies, as shown in Figure 12a, including a significant component at the first (floor) mode frequency, 10.4Hz, leading to a rating >ISO: 10Hz.

The second FLT studied was a small electric Komatsu 15R unit used on the upper level (3000-3U-7) of the same unit. The response for movement of this vehicle along WP1 is shown in figure 12b. Again, this is a smooth floor, and the response was mainly in the first floor mode (9.5Hz) with a rating ISO: 10Hz, 20Hz.

The third FLT (Figure 4b) studied was an electric Toyota machine that was progressively moving loaded pallets from inside floor 3000-3L-8 to the structurally connected external car park (right hand side of Figure 5). This floor surface is unsmoothed concrete, with a construction joint in the car park. Figure 12c shows a response measurement during a single round trip of the FLT, including the sharp transients while passing the joint. This is the strongest response recorded during the measurement campaign, with the FLT clearly exciting a number of vibration modes. The response massively exceeds even the ISO limit (>>ISO: 10Hz) with 1 mm/second RMS velocity.

VCs values for the three FLT examples based on the peak hold spectra are summarized in Table 1 column 10, with the frequency for the governing RMS (closest to VC envelope) given in the table.

Response to fixed machinery within unit

Few of the units tested operated heavy manufacturing machinery, and the example shown is for the two folding presses visible in Figure 4a for which Figure 13 shows time series and peak hold one-third octave spectra. The strong accelerations are short-lived transients but reach peak levels similar to the worst case FLT response. In this case the shape of the spectrum neatly shows that both low and high modes are engaged, and that the lower modal mass of the high modes does not result in higher velocity response.

Response to controlled walking (footfall)

The common denominator and performance benchmark among the measurements is expected to be the standard walking test, with a 100kg pedestrian. For T2000/3000/5000 floors the walking test comprised a sequence of round trips along a designated walking path at specific pacing rates from 90 to 144 paces or beats per minute (bpm), increasing by 6pm each round trip, and prompted by a metronome. Note that most vibration qualification exercises do not require walking faster than 120bpm (a brisk 2Hz pacing rate). The walking paths are indicated on the exemplar floor plans, Figure 5 and figure 6. The responses are examined in some details as they represent response to a standard loading in a narrow range of discrete multi-harmonic frequencies. They are presented in Figure 14-19 and the VCs are summarized in Table 1 column 11. Effects of strong machinery-induced transients not due to walking are deliberately excluded from the peak hold values.

Figure 14 shows a short time series sample of response in 3000-3L-8, the most intensely studied T3000 floor, which behaves very well as a high frequency floor, with the short-lived footfall-generated transients superimposed on the background ambient response. The maximum response occurs elsewhere in the time series when the first mode at 10.5Hz is excited by the sixth harmonic of walking at 102bpm, and the performance just fails VC-A (ISO: 10Hz).

Floor 3000-3L-7 footfall response (not shown) is also impulse-driven but heavily contaminated by other effects in this busy industrial unit and the rating is just within VC-A with a strong 10Hz band (corresponding to first vibration mode). The upper level 3000-3U-7 has very similar performance and is also VC-A.

Figure 15a is the spectrogram of response at the expected most lively point in 5000-1U-10, in the vicinity of reported perceptible vibration response suspected by the tenant to be due to worker footfall. The floor quasi-static response to the harmonics of the (increasing) pacing rate is clear. Apart from the sharp lines after 600 seconds (that are clearly due to machinery), the strong broadband response from 350-550 seconds seems to have the same transient character but is not in time with the footfalls. Close examination of the time series (Figure 15b) shows that the strong response has a different character to the footfall transient.

Observation of the testing equipment used by the tenant showed these not to be the cause, and given the transmissibility illustrated in Figure 8 a possible cause could be a tenant of a unit higher up the stack.

For empty floor 2000-5U-5 (Figure 16), responses are partially obscured by the steady background vibrations in first mode at 12Hz that are clear in the 3D spectrogram. Response is only shown for a point in the bay containing WP1 (Figure 5) for which response in first mode (12Hz) is strongest due to forcing at the fifth-harmonic of the fastest achievable pacing at 144 bpm. This is partly because effective impulse increases with pacing rate (Pavic and Willford, 2005) and partly because there is there is a small component of resonant response due to the fifth harmonic of the pacing rate. The response after 550 seconds is due mainly to walking along WP2 and the rating is ISO solely due to the 12.5Hz band.

Figure 17 for floor 2000-5L-6 shows response levels that clearly increase with pacing rate (larger effective impulse). The result is a rating of VC-A solely due to the first mode response, which occurs in the 12.5Hz band. The free decay from transient excitation is clearest in this example, as illustrated in Figure 17b) for the 98bpm pacing rate.

Figure 18 shows response in the heavily studied 2000-3L-4, which also behaves as a high frequency floor for footfall, but only the first cycle of response due to each footstep (WP1, Figure 5) is noticeable above the background noise. The rating is VC-A solely due to steady noise at 19Hz, which falls in the 20Hz band. The noise source is unknown (the unit is completely empty) but given the transfer mobility result from Figure 8 it is possible the source could be in the unit below which could not be accessed. Footfall has little effect on this floor and the first mode is only weakly excited, which is consistent with the anomalous high modal mass.

Finally, Figure 19 shows response to footfall in the only large ground level floor studied, 2000-1L-3. Being slab-on-grade, no modes were observed in the 10-40Hz and the one-third octave spectrum is uniform with mild enhancement at 10Hz, for VC-D rating. There are no machines in this unit, but on occasion (not during the walking) the ambient response reaches VC-B due to a strong signal at 10Hz from the structurally connected neighbouring unit that uses heavy manufacturing machinery.

Ambient response

Ambient vibration levels were obtained for all ten floors in terms of one-third octave velocity spectra during periods without specific vibration sources such as machinery, vehicles or heavy footfall i.e. the background noise for a unit, but obtained at the most lively point on the floor, such as mid-bay. RMS averaging was used with T=10 seconds (Eriksson 1996) and ratings are shown in Table 1 column 9.

For the largest floor tested (5000-1U-10, Figure 4d), the average floor vibration performance is (just) VC-A due to steady machinery–induced vibration in the 12.5Hz band illustrated in Figure 15.

All four T3000 floors have governing ambient response in the 10Hz band due to the first floor vibration mode. For lower and upper floors of 3000-3L/U-7 performance is at VC-B due to broadband response around the floor first mode. Even though mode properties are similar in either floor, 3000-3U-7 is a whole vibration class ‘worse’ than the lower floor.

The performance for 3000-3L-8 (Figure 4b) is VC-C. This floor is used as a warehouse and is otherwise empty.

Floor 3000-5L-9 (Figure 4c) is the highest of its type tested and also the worst performing, with peak hold worse than ISO. This is surprising given that the precision machining operations in this unit in operation would normally require a low-vibration environment.

All four T2000 floors have either weak or no internal vibration-generating activities and average response is VC-B. For 2000-3L-4 ambient vibration, maximum at 20Hz is almost as strong as walking (VC-B vs. VC-A), consistent with the unusually high modal mass values obtained by EMA. For other T2000 units response at the first mode frequency is largest. For the 2000-5L/U-6 pair response is slightly stronger in the upper level.

Summary of performance

Based on the set of measurements and the summary of Table 1, the following observations can be made about the relationship of vibration performance with factors such as type and size of unit, location, and sources of vibration.

In terms of vibration performance, there is little to choose between T3000 and T2000 floors whose ambient response is governed by differing factors. The largest floor (5000-1U-10, Figure 4d, Figure 15) performed worst, with no obvious internal cause. Otherwise, floors at higher levels appear to have stronger background vibration levels and floors at ground level had the lowest vibration levels for all forms of internal excitation.

Forklift trucks produced by far the worst effect among all the machinery-induced responses by an order of magnitude, judged by performance in 3000-3L-7 and 3000-3L-8, with worst-case velocities reaching 1mm/second. Best strategy for mitigating such effects is evidently a smooth floor free of construction joints. Transient loads by other machinery such as metal presses distribute energy across the spectrum so modal response is limited.

Although not described due to lack of space, from observing vehicle movements and operations in neighbouring units, it appears that transmission from and across the structurally linking roadways is apparently negligible and can be disregarded. On the other hand the transmissibility test showed the potential for vibration transmission between levels.

Walking tests provide a means of comparing performance of floors by walking the same way in equivalent locations on different floors. For the T3000 floors footfall-induced vibrations were consistently around the VC-A/ISO boundary, while T2000 floors all performed in VC-A range, with the exception of 2000-5U-5. The largest floor with the largest modal mass had the best response to footfall (when external effects are excluded).

Conclusions

The aim of the modal analyses and vibration surveys was to characterise the vibration environment according usage and floor structural layout and to rationalise this behaviour against the modal floor modal properties. The study was intended to support a performance-based approach to floor selection, so that tenants and management could make best choice of unit for a particular usage profile. All floor first modes had frequencies above 9Hz and modal masses at least 60×10^3kg and with the exception of a ground floor slab (on grade) rated VC-B or worse for a single pedestrian. Modes above 30Hz had low modal mass (as low as 28×10^3 kg) but were not relevant for vibration performance. Surprisingly, the nominally similar T2000 units had widely varying modal and operational performance.

Should a low vibration environment be required, ground floor units would be preferable, with neighbours above or below not using heavy machinery or fork-lift trucks (FLTs). Worst performance was observed with operation of FLTs, particularly those with stiff tyres moving over rough concrete with construction joints.

With a trend to more 'high tech' commercial operations in such industrial complexes, the issue of vibration serviceability will require careful consideration by prospective tenants and building management. Where smaller spans or floors at ground level are not available, specific evaluations would be advisable for vibration-sensitive activities. The use of vibration criteria A though E, widely used in vibration sensitive electronic/optical facilities seems to be appropriate for the type of structure studied here.

Even so, tenants with vibration-sensitive operations should use lower floors. This may be obvious to structural engineers but it is not obvious to many facility designers. Likewise the effects of machinery and vehicles can be mitigated by careful placement of fixed equipment and ensuring floors smooth and bump-free. Given the transfer mobility observed between two upper levels of a stack and evidence from two of the floors studied, there could be impact of strong vibration sources in higher or lower floors.

References

American National Standards (1986). Specification for Octave-Band and Fractional-Octave-Band Analog and Digital Filters. ANSI S1.11-1986.

Amick, c.H., Hardash, S. Gillett, P., Reaveley, R.J., (1991). Design of stiff, low-vibration floor structures. Proceedings of the International Society for Optical Engineering (SPIE), 1619, 180-191.

Amick, C. H., Gendreau, M., Busch, T., Gordon, C. G., (2005). Evolving criteria for research facilities: I – Vibration. In: SPIE Conference 5933: Buildings for Nanoscale Research and Beyond,

Brownjohn, J. M. W., Hao, H., and Pan, T.-C., (2001). Assessment of structural condition of bridges by dynamic measurements. Nanyang Technological University, Applied Research Project RG 5/97. Singapore

Brownjohn, J.M.W., Pavic, A. (2006). Vibration control of ultra-sensitive facilities. Proceedings of the Institution of Structural Engineers, Structures and Buildings 159(SB1), 1-12.

Brownjohn, J.M.W., Pavic, A. (2007). Experimental methods for estimating modal mass in footbridges using human-induced dynamic excitation. Engineering Structures 29(11), 2833-2843.

Brownjohn, J. M. W., Middleton, C.J. (2009). Response of high-frequency floors: A literature review. Engineering Structures 30 1548-1559

Dallard P, Fitzpatrick A, Flint A, Low A, Ridsell smith R, The Millennium Bridge, London. Problems and solutions. The Structural Engineer 79(8), 2001, 15-17.

Ehland, A., (2009). Vibrations of precast and partially prestressed floor systems under moving loads. D. Phil thesis, Department of Engineering Science, University of Oxford.

Ehland, A., Williams, M. S., Blakeborough, A., (2010). Dynamic load model for fork-lift trucks. Engineering Structures 32(9), 2693-2701.

Eriksson, P.-E., (1994). Vibration of low-frequency floors - dynamic forces and response prediction. PhD Thesis. Chalmers University of Technology, Göteborg, Sweden.

Ewins, D. J. (2000). Modal Testing: Theory, Practice and Application. Research Studies Press.

Highways Agency (2001). Design Manual For Roads and Bridges Design Manual For Roads And Bridges Volume 1 Section 3 Highway Structures: Approval Procedures and General Design General Design Part 14 BD 37/01.

Internatinal Standards Organisation, (2003). Mechanical vibration and shock – Evaluation of human exposure to whole-body vibration – Part 2: Vibration in buildings (1Hz to 80Hz)/ ISO 2631-2:2003.

Pan, T. C., Mita, A., (2001). Vehicle-Induced Floor Vibrations in a Multistory Factory Building. Journal of Performance of Constructed Facilities 15, No. 2**,** 54-61.

Pavic, A., Willford, M., (2005). Vibration serviceability of post-tensioned concrete floors. Appendix G in Post-Tensioned Concrete Floors Design Handbook - Technical Report 43. 99-107.

Rainer, J.H., Swallow, J.C., Dynamic behaviour of a gymnasium floor. Canadian Journal of Civil Engineering 13(3), 270-277.

Richardson, M. H., Formenti, D. L., (1982). Parameter estimation from frequency response measurements using rational fraction polynomials. Proceedings, First International Modal analysis Conference, 167-181

Rogers. D., Thompson, R., (2000). Liverpool stand gets a red card. Construction News, 10 August.

SCOSS, (1988). Seventh report of the Committee for the two years endiing July 1987. Standing Comitte on Structural Safety, EA/88/4.

The Steel Construction Institute (2009). Design of Floors for Vibration: A new Approach (Revised Edition, February 2009, particularly Appendix C).

Vibrant Technology Inc., (2003). ME'scope VES 4.0, Volume 1 - Tutorial.

Xia, H., Chen, J., Wei, P., Xia, C., De Roeck, G., De Grande G., (2009). Experimental investigation of railway train-induced vibrations of surrounding ground and a nearby multi-story building. Earthquake Engineering and Engineering Vibration 8, 137-148.

Table 1 Floors tested: type, usage, modal parameter estimates and vibration ratings.

Floor	Usage	Low modes			High modes			Vibration criteria (VC), relevant figure and peak band centre frequency (Hz)		
		f / Hz	m /10^3kg	ζ/%	f /Hz	m /10^3kg	ζ/%	ambient	FLT	Walking
2000-1L-3	storage	-	-		-	-		-		D: 10Hz Figure 19
2000-3L-4	empty	12.9	180 /130	2.3	16.9	180	2.5	B: 20		A: 20 Figure 18
2000-5U-5	empty	11.6	120	3.0	15	79	4.8	B: 12.5		>ISO: 12.5 Figure 16
2000-5L-6	instrument assembly	12.4	80	2.4	19.9	150	3.7	B: 12.5		A: 12.5 Figure 17
2000-5U-6	storage	12.4	-	2.4	n/a	n/a	n/a	B: 12.5		-
3000-3L-7	metalwork	10.4 /12.2	60 /150	3.8/ 3.1	36.4	38	3.9	B: 10	>ISO Figure 12a	A: 10
3000-3U-7	storage	9.5 /10.7	120 /88	3.2/ n/a	39.1	45	4.4	B: 10	ISO Figure 12b	A: 10
3000-3L-8	warehouse	10.3 /12.8	120 /200	3.4/ 2.9	37.1	35	3	C: 10	>>ISO Figure 12c	ISO: 10 Figure 14
3000-5L-9	micro-electronics manufacture	9.6	n/a	n/a	37.3	28	4.6	A: 10		A: 10
5000-1U-10	optics assembly & test	11.1 /12.5	200 /200	1.5 2.3	35.5	36	2.2	A: 12.5		B: 12.5

n/a modal property not estimated

Figure 1: S1 plan at ground level. Section at a-a is shown in Figure 2. There are six units of two levels in each of the blocks indicated.

Figure 2: S1 side sectional elevation for stack of T5000 + 2×T3000 units (labelled SS5000/3000) at a-a in Figure 1. Access roads at levels 1,3 and 5 are to right.

a) View behind row of T2000 units
b) Empty 2000-5U-5. Engineer (in oval) indicates size of unit
c) Block of two detached T3000 units
d) Empty 2000-3L-4 towards loading bay

Figure 3: S1 external and internal views.

a) Metal folding machines in 3000-3L-7
b) Forklift truck (FLT) in 3000-3L-8
c) Precision machining in 3000-5L-9 (some details obscured)
d) Walking test in 5000-1U-10 (instrument assembly/test facility)

Figure 4: Example occupancy, industrial usage and operational performance environment

Figure 5: Arrangement of 3000-3L-8 showing point mobility measurement point (dot) and walking paths WP1,2 (solid lines). One bay shows as cutaway a typical arrangement of hollow core planks spanning 7.5m. Internal main beams span 6m and 18m, car park span is 12m.

Figure 6: Arrangement of 2000-3L-4 (right hand unit of the pair of semi detached units) showing measurement points (dots) and walking paths WP1,2 (solid lines). One bay in left hand unit shows as cutaway a typical arrangement of hollow core planks spanning up to 12m

a) T2000 floors
b) T5000/3000 floors

Figure 7: Point mobility frequency response functions for most lively mid-bay locations.

a) Driving point mobility (inertance) between 2000-5L-6 (input) and 2000-5L-6 (response)
b) Transfer mobility (inertance) between 2000-5L-6 (input) and 2000-5U-6 (response)

Figure 8: Mobility measurements at lower and upper levels in T2000 by hammer testing.

Figure 9: Hollow core plank representation as grillage.

FEA: 12.5Hz
EMA 12.9Hz, m=180 $\times 10^3$ kg
FEA: 16.5Hz
EMA 16.9Hz, m=180 $\times 10^3$ kg

Figure 10 Analytical (FEA) modes matching experimental (EMA) modes for T2000 floor 2000-3L-4. See

Figure 6 for location of point ‘A’.

FEA: 9.8Hz (EMA 10.3Hz, m=120 $\times 10^3$ kg)

FEA: 12.7Hz (EMA 12.8Hz)

Figure 11: Two analytical (FEA) modes that match experimental (EMA) modes for T3000 floor 3000-3L-8.

a) FLT in 3000-3L-7 (>ISO)
b) FLT in 3000-3U-7 (ISO)
c) FLT in 3000-3L-8 (>>ISO)

Figure 12: Response to FLTs onT3000 floors as time series and peak-hold one-third octave spectra.

Figure 13: Response to fixed internal machinery: metal folding press in 3000-3L-7 (ISO: 32Hz).

Figure 14: Impulsive nature of floor response to walking (WP2,

Figure 5**)** in 3000-3L-8 (ISO: 10Hz).

a) pairs of bands throughout are return trips along walking path

b) footfall transients and example of strong response to unknown excitation

Figure 15: Spectrogram and 10-second time series of midbay acceleration response in 5000-1U-10 during walking test.

a) Response low-pass filtered at 40Hz.

b) 3D spectrogram for a)

Figure 16: Walking tests in 2000-5U-5 (>ISO: 12.5Hz).

a) Response low pass filtered at 40Hz. Response increases with pacing rate due to increasing effective impulse

b) Zoom into a) showing classical high frequency floor response and lack of resonance build-up

Figure 17: Walking tests in 2000-5L-6 (VC-A: 12.5Hz).

a) Time series for complete walking record

b) 3D spectrogram

Figure 18: Walking test (WP1,

Figure 6) in 2000-3L-4 (VC-A: 20Hz), shows impulsive response buried in ambient excitation at 20Hz.

Figure 19: Walking test in 2000-1L-3 (VC-D: 10Hz)

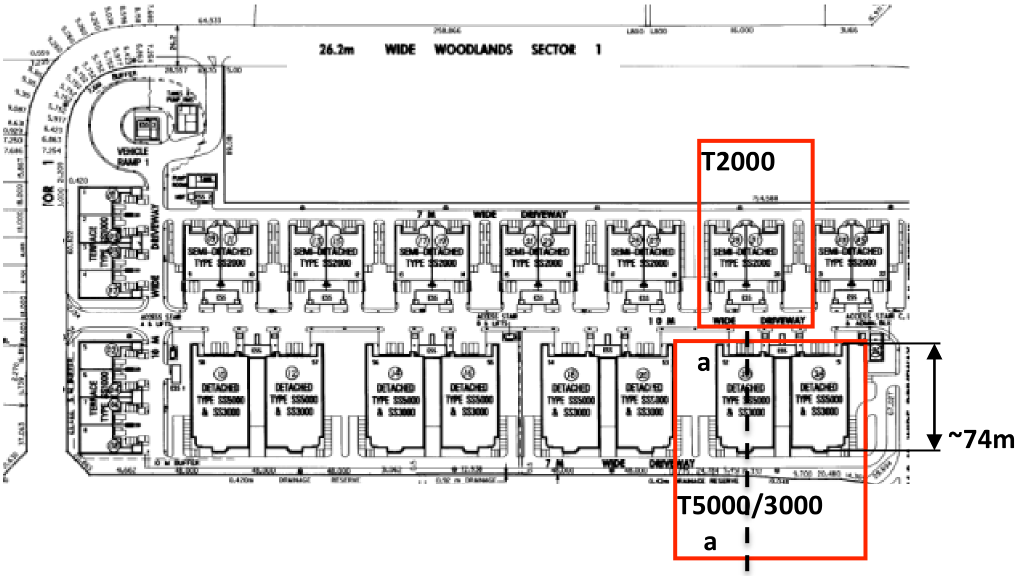
26.2m WIDE WOODLANDS SECTOR 1
T2000
7 M WIDE DRIVEWAY
SEMI-DETACHED TYPE SS2000
10 M WIDE DRIVEWAY
DETACHED TYPE SS5000 & SS3000
~74m
a
T5000/3000
a

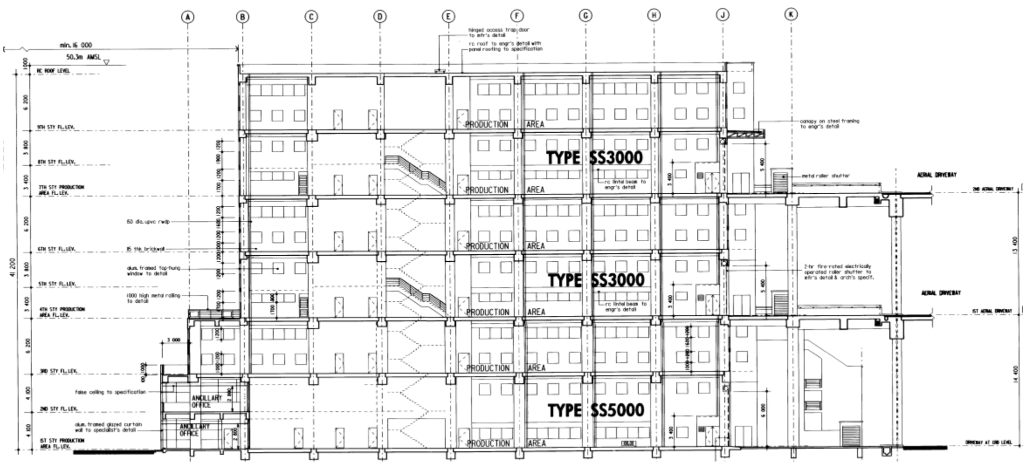
A
B
C
D
E
F
G
H
J
K
TYPE SS3000
TYPE SS3000
TYPE SS5000
PRODUCTION AREA
PRODUCTION AREA
PRODUCTION AREA
PRODUCTION AREA
PRODUCTION AREA
PRODUCTION AREA
ANCILLARY OFFICE
ANCILLARY OFFICE




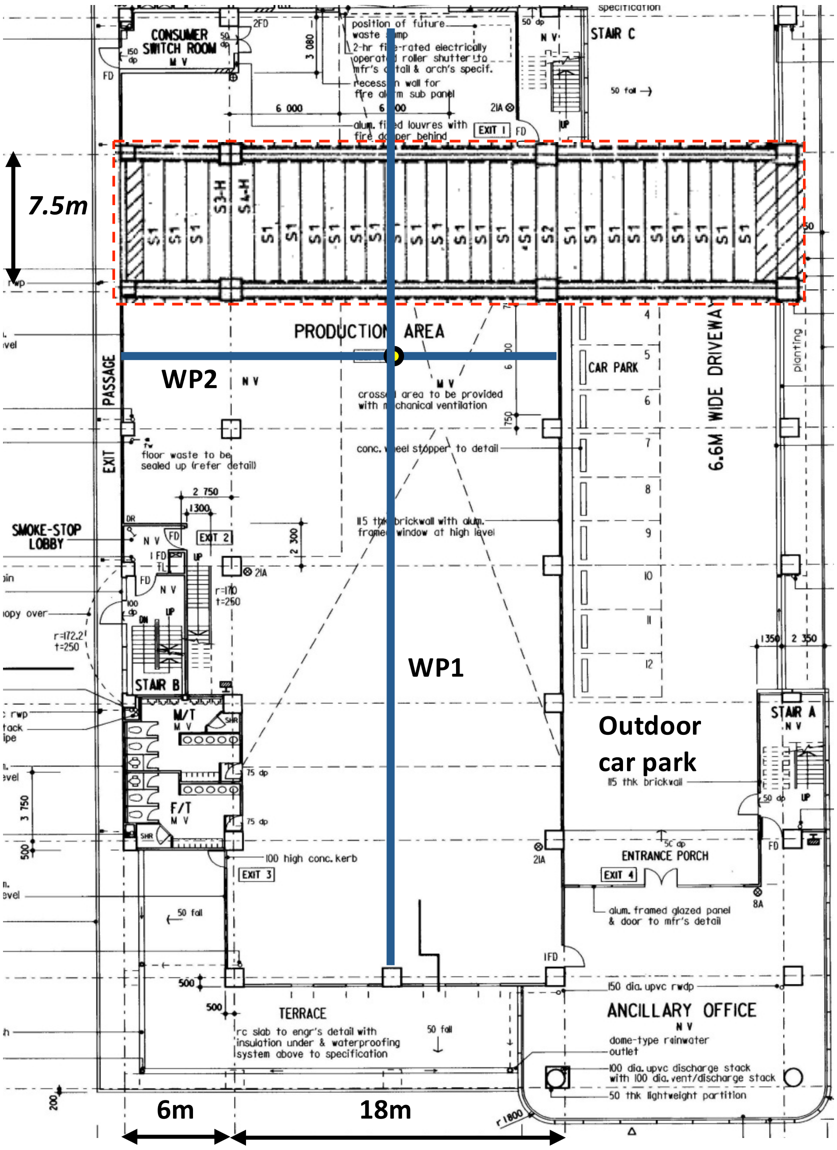
7.5m
CONSUMER SWITCH ROOM
STAIR C
PRODUCTION AREA
WP2
WP1
PASSAGE
EXIT
SMOKE-STOP LOBBY
STAIR B
M/T
F/T
CAR PARK
6.6M WIDE DRIVEWAY
Outdoor car park
STAIR A
ENTRANCE PORCH
TERRACE
ANCILLARY OFFICE
6m
18m

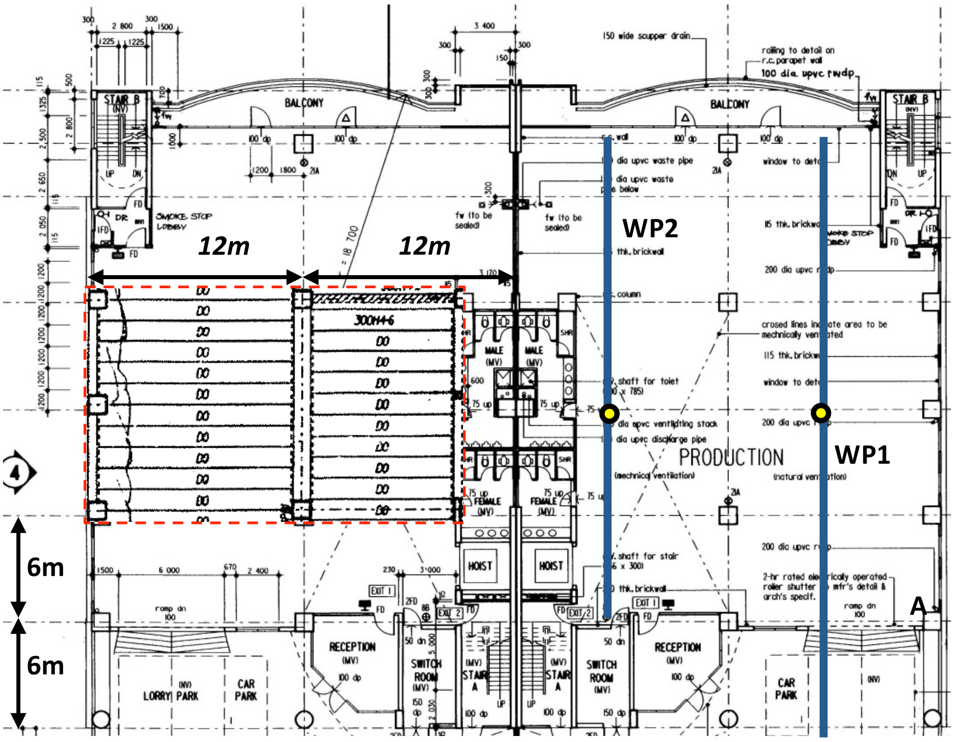

12m
12m
WP2
WP1
6m
6m
BALCONY
BALCONY
STAIR B
STAIR B
PRODUCTION
MALE
MALE
FEMALE
FEMALE
HOIST
HOIST
RECEPTION
RECEPTION
SWITCH ROOM
SWITCH ROOM
STAIR A
STAIR A
LORRY PARK
CAR PARK
CAR PARK
A

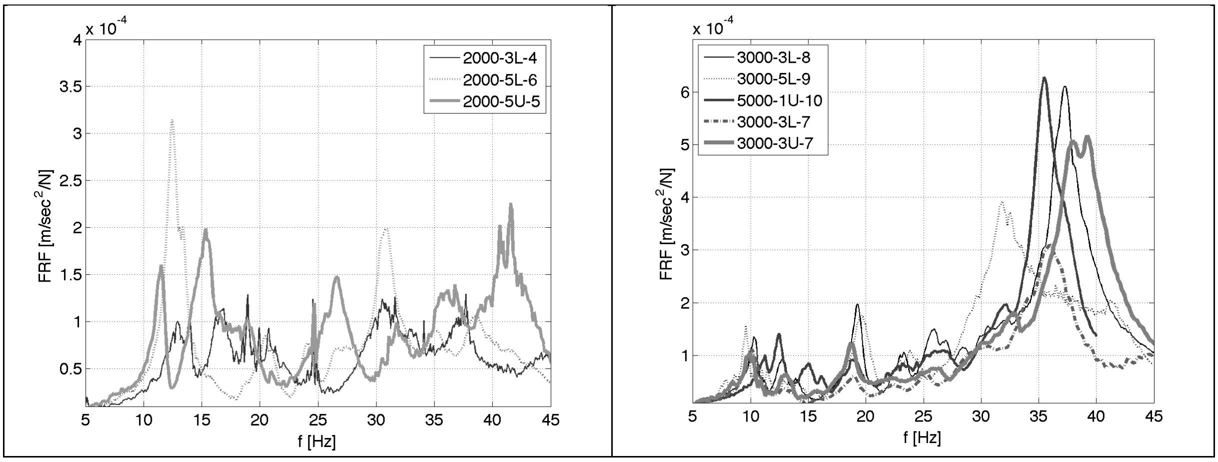

x 10^-4
FRF [m/sec^2/N]
f [Hz]
2000-3L-4
2000-5L-6
2000-5U-5
3000-3L-8
3000-5L-9
5000-1U-10
3000-3L-7
3000-3U-7

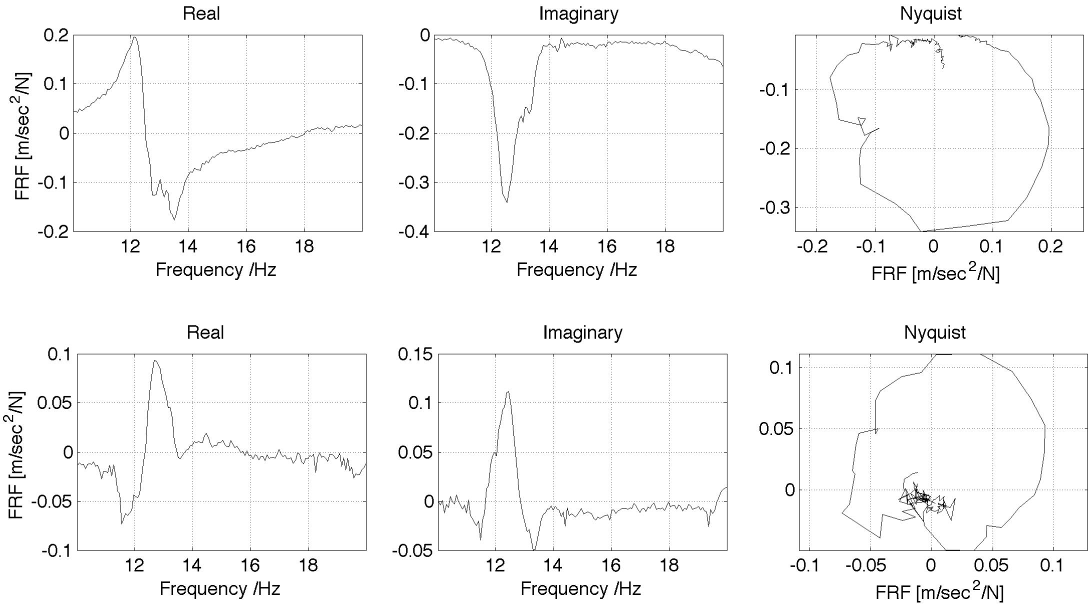
Real
Imaginary
Nyquist
FRF [m/sec^2/N]
Frequency /Hz
FRF [m/sec^2/N]
Real
Imaginary
Nyquist
FRF [m/sec^2/N]
Frequency /Hz
Frequency /Hz
FRF [m/sec^2/N]

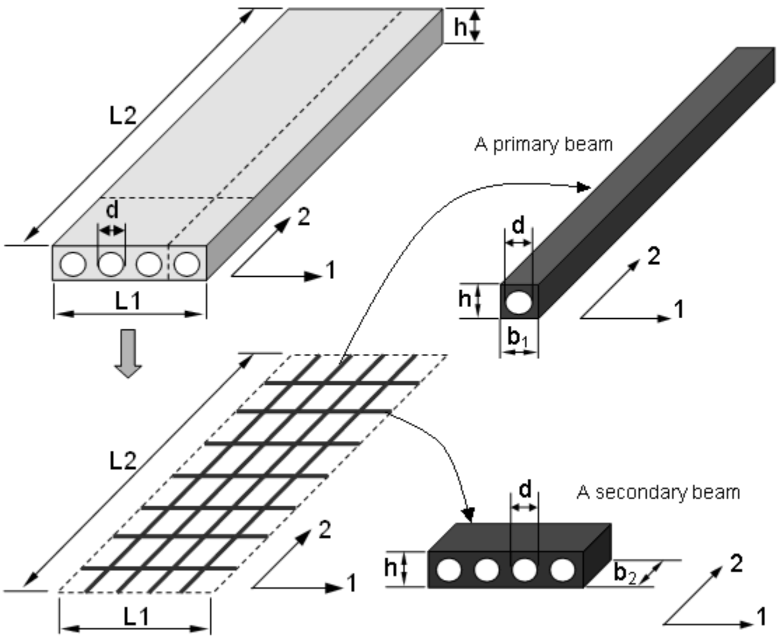
h
L2
d
2
1
L1
A primary beam
d
h
b1
2
1
L2
d
A secondary beam
2
h
b2
2
1
L1
1

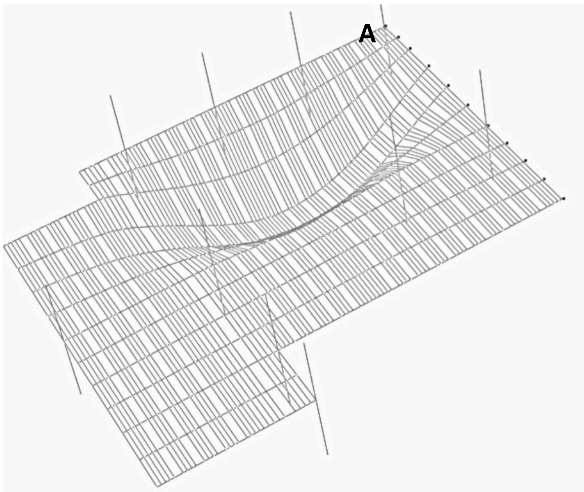

FEA: 12.5Hz

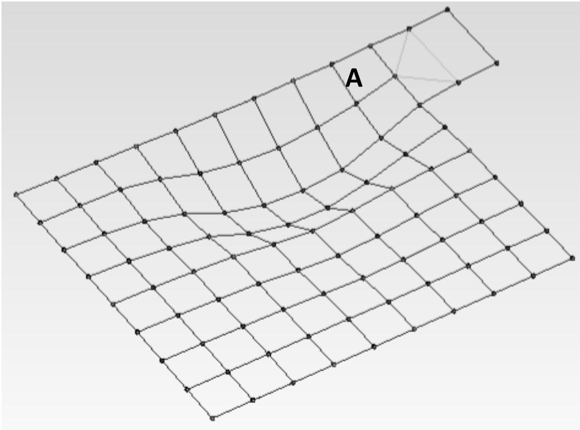

EMA 12.9Hz, m=180 $\times 10^3$ kg

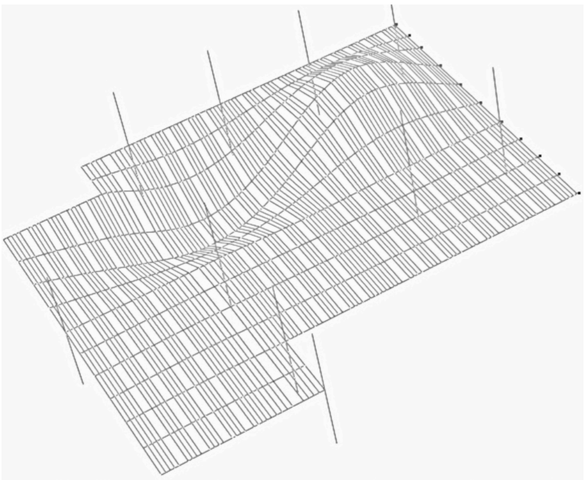

FEA: 16.5Hz

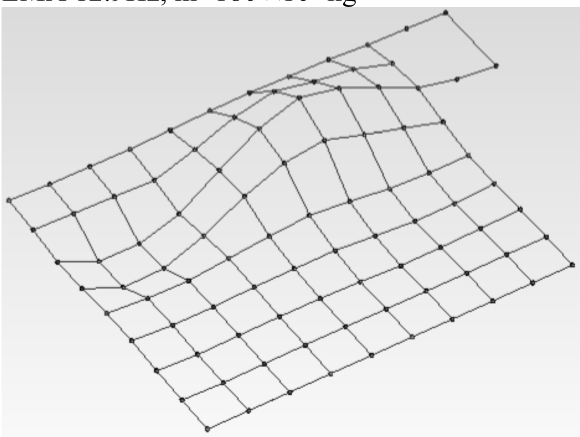

EMA 16.9Hz, m=180 $\times 10^3$ kg

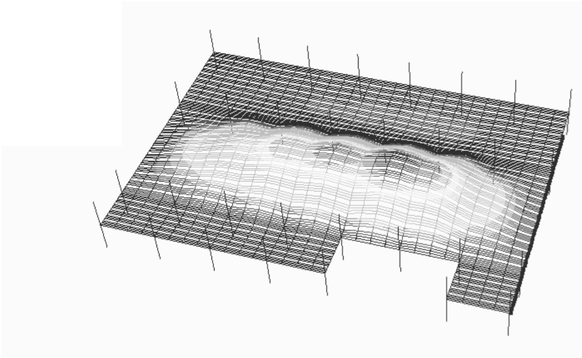

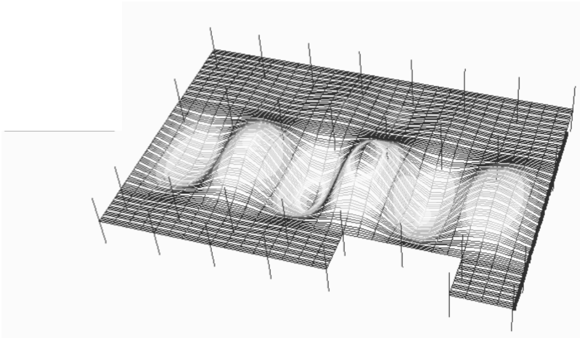

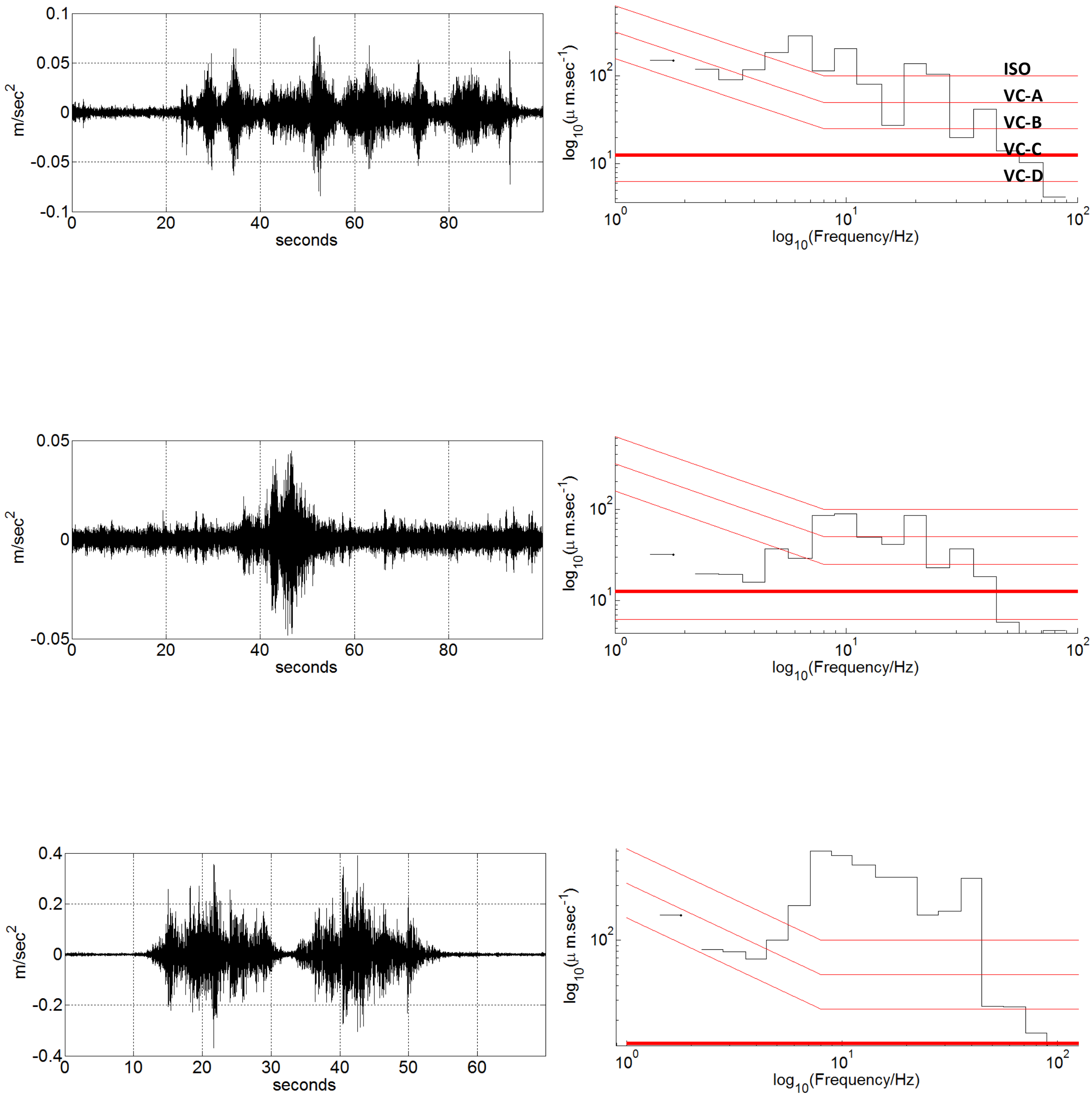
m/sec^2
seconds
$\log_{10}(\mu$ m.sec$^{-1})$
$\log_{10}$(Frequency/Hz)
ISO
VC-A
VC-B
VC-C
VC-D

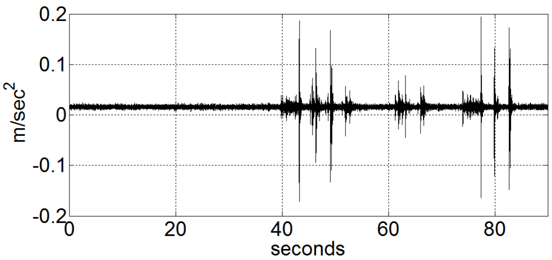
0.2
0.1
0
-0.1
-0.2
m/sec2
0
20
40
60
80
seconds

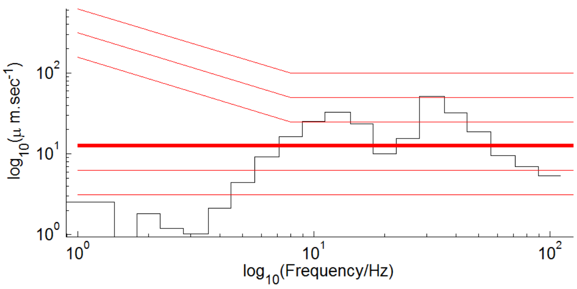
10^2
10^1
10^0
log10(μ m.sec-1)
10^0
10^1
10^2
log10(Frequency/Hz)

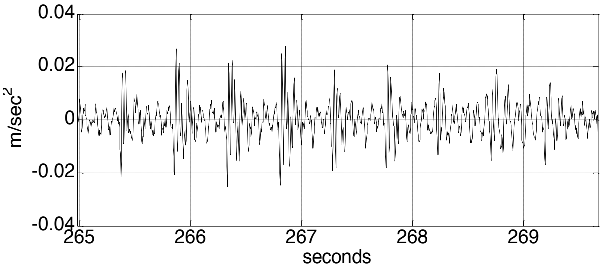
0.04
0.02
0
-0.02
-0.04
m/sec²
265
266
267
268
269
seconds

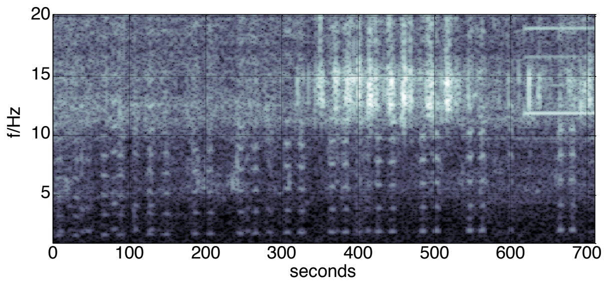
f/Hz
20
15
10
5
0
100
200
300
400
500
600
700
seconds

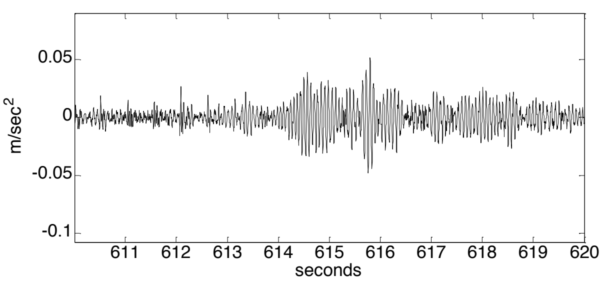
m/sec^2
0.05
0
-0.05
-0.1
611
612
613
614
615
616
617
618
619
620
seconds

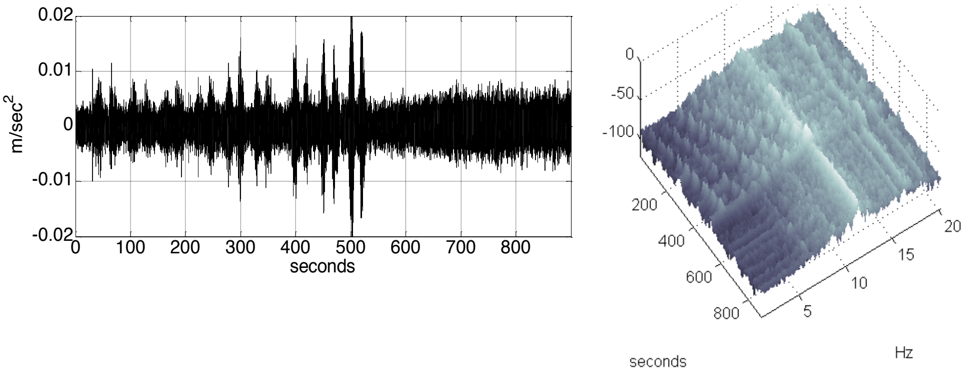
0.02
0.01
0
-0.01
-0.02
m/sec²
0
100
200
300
400
500
600
700
800
seconds
0
-50
-100
200
400
600
800
seconds
5
10
15
20
Hz

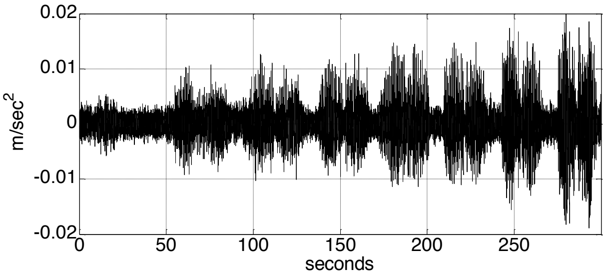
0.02
0.01
0
-0.01
-0.02
m/sec^2
0
50
100
150
200
250
seconds

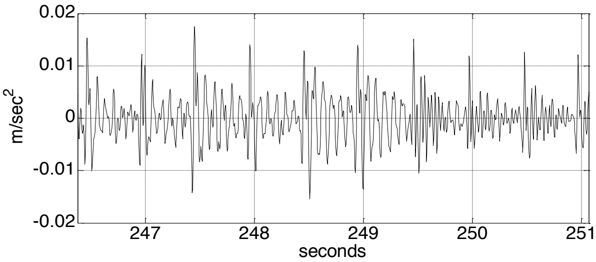
0.02
0.01
0
-0.01
-0.02
m/sec^2
247
248
249
250
251
seconds

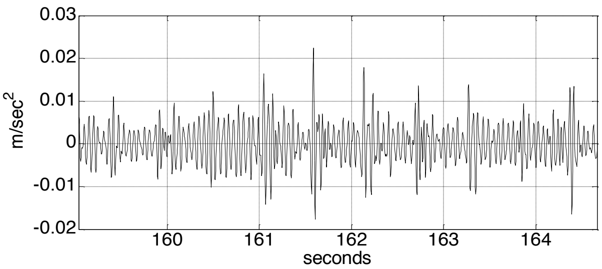
0.03
0.02
0.01
0
-0.01
-0.02
m/sec2
160
161
162
163
164
seconds

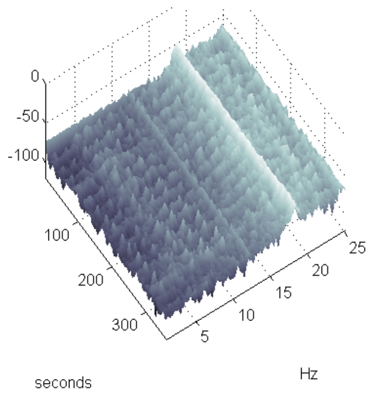
0
-50
-100
100
200
300
5
10
15
20
25
seconds
Hz

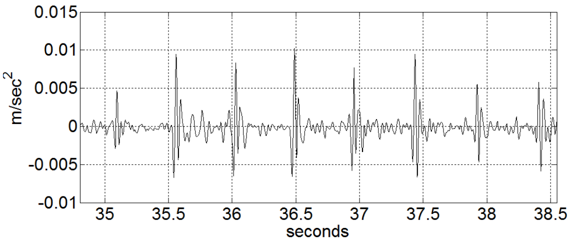
0.015
0.01
0.005
0
-0.005
-0.01
m/sec2
35
35.5
36
36.5
37
37.5
38
38.5
seconds

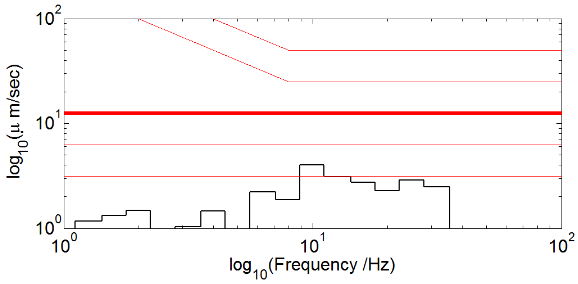
10^2
10^1
10^0
log10(μ m/sec)
log10(Frequency /Hz)